The EMBO Journal (2012) 31, 3147–3156 | © 2012 European Molecular Biology Organization | All Rights Reserved 0261-4189/12
www.embojournal.org

THE EMBO JOURNAL

Coordinated signal integration at the M-type potassium channel upon muscarinic stimulation

Anastasia Kosenko[1], Seungwoo Kang[1], Ida M Smith[1], Derek L Greene[1], Lorene K Langeberg[2], John D Scott[2] and Naoto Hoshi[1,*]

[1]Department of Pharmacology, University of California, Irvine, CA, USA and [2]Department of Pharmacology, Howard Hughes Medical Institute, University of Washington, Seattle, WA, USA

Several neurotransmitters, including acetylcholine, regulate neuronal tone by suppressing a non-inactivating low-threshold voltage-gated potassium current generated by the M-channel. Agonist dependent control of the M-channel is mediated by calmodulin, activation of anchored protein kinase C (PKC), and depletion of the phospholipid messenger phosphatidylinositol 4,5-bisphosphate (PIP2). In this report, we show how this trio of second messenger responsive events acts synergistically and in a stepwise manner to suppress activity of the M-current. PKC phosphorylation of the KCNQ2 channel subunit induces dissociation of calmodulin from the M-channel complex. The calmodulin-deficient channel has a reduced affinity towards PIP2. This pathway enhances the effect of concomitant reduction of PIP2, which leads to disruption of the M-channel function. These findings clarify how a common lipid cofactor, such as PIP2, can selectively regulate ion channels.

The EMBO Journal (2012) **31,** 3147–3156. doi:10.1038/emboj.2012.156; Published online 29 May 2012
Subject Categories: signal transduction; neuroscience
Keywords: calmodulin; protein complex; protein kinase C; signal transduction; voltage-gated potassium channel

Introduction

The M-current is generated by a group of low-threshold voltage-gated potassium channels encoded by the KCNQ gene family (KCNQ2, 3, 4, and 5) (Jentsch, 2000; Delmas and Brown, 2005). These subunits form heteromeric M-channels that control neuronal excitability and firing frequency. Accordingly, mutations in KCNQ genes underlie congenital excitatory neuropathological conditions and epilepsies including benign familial neonatal convulsions (Cooper and Jan, 1999; Jentsch, 2000).

M-channels set the tone for neuronal activity. They generate the medium after-hyperpolarization currents that regulate intervals of neuronal firing (Peters *et al*, 2005). In fact, the M-channel can be considered to function as a band pass filter (Hu *et al*, 2009) as it optimizes the most effective frequency for neuronal reactivity to the theta frequency (6–10 Hz). This particular frequency of neuronal activity is important for inducing long-term potentiation, and is therefore critical for learning and memory (Buzsaki, 2002). In addition, activation at a near resting membrane potential counteracts the accumulation of excitatory postsynaptic potentials (Delmas and Brown, 2005; George *et al*, 2009; Shah *et al*, 2011), which triggers firing of action potentials at the axon initial segment where M-channels are clustered (Pan *et al*, 2006; Shah *et al*, 2008). Various neurotransmitters annul M-currents to lower the threshold for action potential firing (Marrion, 1997). A classic example of this is the action of acetylcholine (Brown and Adams, 1980). Stimulation of the m1 muscarinic acetylcholine receptor activates phospholipase C (PLC): an enzyme that catalyses the breakdown of PIP2 to generate diacylglycerol (DAG) and inositol trisphosphate. This combination of second messengers activates protein kinase C (PKC) and increases cytosolic calcium, respectively. Although each effector acts through a distinct mechanism, each of these PLC-mediated signalling events is sufficient to suppress the M-current (Gamper and Shapiro, 2003; Hoshi *et al*, 2003; Suh *et al*, 2006). For example, PIP2 has been identified as an essential cofactor for the M-channel function. Thus, depletion of PIP2 induced by PLC activation can suppress the M-current (Suh and Hille, 2002; Zhang *et al*, 2003; Winks *et al*, 2005). Local activation of PKC is required for muscarinic suppression of the M-current (Hoshi *et al*, 2005) and is controlled by the kinase anchoring protein, AKAP79/150 (Hoshi *et al*, 2003). Likewise, the release of calmodulin from the M-channel complex has been demonstrated to reduce the M-current (Yus-Najera *et al*, 2002; Shahidullah *et al*, 2005). Interestingly, all these candidate molecules: PIP2, AKAP79/150 and calmodulin, bind in close proximity to each other at the C-terminal tail of the M-channel as a macromolecular complex (Yus-Najera *et al*, 2002; Hoshi *et al*, 2003; Zhang *et al*, 2003; Delmas and Brown, 2005; Hernandez *et al*, 2008). Hence, there is reason to suspect synergistic regulation by these second messengers or effector proteins. However, the molecular interplay between these cofactors is not well understood.

In this report, we demonstrate that PKC phosphorylation of the KCNQ2 subunit drives dissociation of calmodulin from the cytoplasmic tail of the channel. Consequently, the KCNQ2 subunit has both lower affinity for PIP2 and a reduced channel activity. Hence, the sequential and synergistic coupling of these factors specifies how ubiquitous signalling molecules such as PIP2 can be organized to selectively modulate the M-current.

Results

PKC phosphorylation at serine 541 of KCNQ2 sensitizes the muscarinic suppression of the KCNQ2 channel

M-currents were recorded from rat superior cervical ganglion (SCG) neurons using perforated patch technique. The

*Corresponding author. Department of Pharmacology, University of California, Irvine, 360 Med Surge II, Irvine, CA 92697, USA.
Tel.: +1 949 824 0969; Fax: +1 949 824 4855; E-mail: nhoshi@uci.edu

Received: 19 December 2011; accepted: 25 April 2012; published online: 29 May 2012

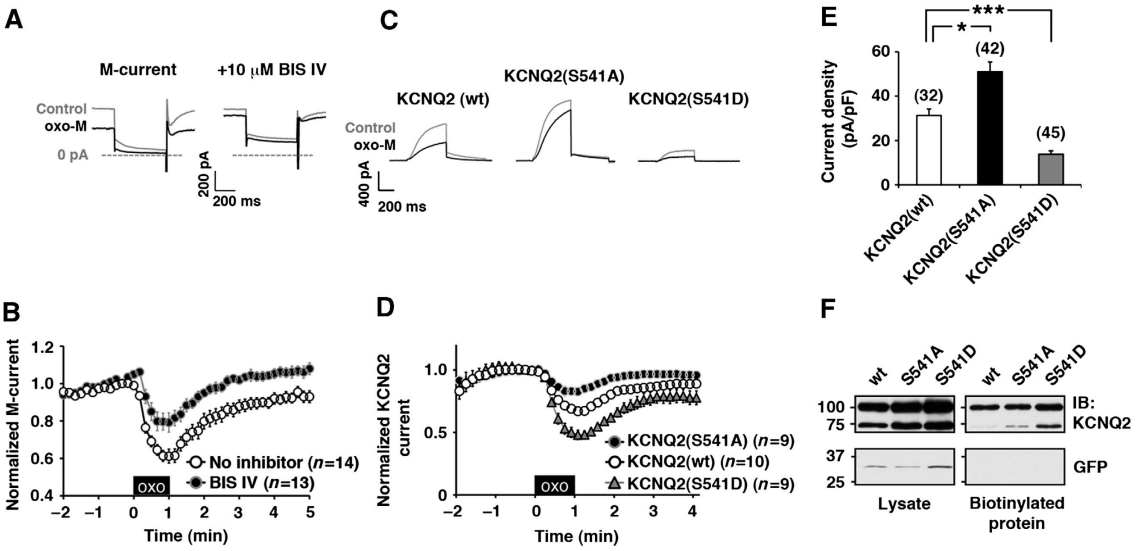

Figure 1 PKC activation sensitizes muscarinic suppression of the M-current via phosphorylation of S541 of KCNQ2 subunit. (**A**, **B**) Perforated patch-clamp recordings from rat SCG neurons showing muscarinic suppression of the M-current induced by 0.1 μM oxo-M is attenuated by 10 μM bisindolylmaleimide IV (BIS IV). (**A**) Current traces showing M-current suppression induced by oxo-M and its attenuation by BIS IV. (**B**) Pooled data showing muscarinic suppression of the M-current. Amplitudes of the M-currents are normalized to those at $t=0$. The black box indicates the presence of oxo-M. (**C**, **D**) Whole-cell patch-clamp recordings from transiently transfected CHO hm1 cells showing muscarinic suppression of wild-type KCNQ2 and its S541 mutants induced by 0.1 μM oxo-M. (**C**) Current traces for KCNQ2 channels and their muscarinic suppressions. (**D**) Pooled data showing oxo-M responses of wild-type KCNQ2, KCNQ2 (S541A), and KCNQ2 (S541D). Amplitudes of the KCNQ2 currents are normalized to those at $t=0$. (**E**) Current densities of wild-type KCNQ2, KCNQ2 (S541A), and KCNQ2 (S541D). $*<0.05$, $***<0.001$ calculated by nonparametric ANOVA followed by *t*-test. (**F**) Cell surface biotin labelling of wild-type KCNQ2, KCNQ (S541A), and KCNQ2 (S541D) (top panels), and of cytosolic GFP (lower panels). A representative blot from four independent experiments is shown. Error bars indicate s.e.m. Figure source data can be found with the Supplementary data.

M-current was suppressed by the application of a muscarinic agonist, oxotremorine-M (oxo-M) (Figure 1A and B; 61 ± 4% at $t=1$ min, $n=14$). This muscarinic suppression was attenuated by bisindolylmaleimide IV (BIS IV) (Figure 1A and B; 79 ± 5%, $n=13$), which we have previously shown to be an effective inhibitor of PKC when it is anchored to the channel via AKAP79/150 (Hoshi *et al*, 2010). Further support for involvement of PKC phosphorylation of KCNQ2 subunits was provided by analysis of KCNQ2 subunits with mutations at S541, a previously identified PKC phosphorylation site (Hoshi *et al*, 2003). Two mutations were produced: an alanine substitution of S541, KCNQ2 (S541A), which lacks an acceptor for PKC phosphorylation, and an aspartate substitution, KCNQ2 (S541D), which mimics phosphorylation. The oxo-M responses of these KCNQ2 channels were measured in transiently transfected Chinese hamster ovary cells that stably express human muscarinic m1 receptor, CHO hm1 cells (Figure 1C and D). The KCNQ2 (S541A) channel exhibited a reduced response to oxo-M (82.7 ± 2.7%, $n=9$). Subsequent application of BIS IV had no additional effect on the muscarinic suppression of this current (83.4 ± 3.6%, $n=11$, $P=0.88$). This is consistent with the removal of a functionally relevant target substrate for PKC. In contrast, recordings of KCNQ2 (S541D) mutant channels exhibited more pronounced suppression when compared with the wild-type channel (Figure 1D; $n=9$). These results support the hypothesis that PKC phosphorylation sensitizes muscarinic suppression.

Furthermore, current densities were increased in cells expressing KCNQ2 (S541A) when compared with cells expressing the wild-type channel (Figure 1E; $n=42$ and $n=32$, respectively). In contrast, KCNQ2 (S541D) displayed reduced current density (Figure 1E; $n=45$). Since some KCNQ2 mutants undergo abnormal membrane trafficking (Jentsch, 2000; Etxeberria *et al*, 2008), the surface protein amounts of these KCNQ2 variants were validated by extracellular biotin labelling assays. All three versions of KCNQ2 channels showed equivalent biotinylation when expressed in CHO hm1 cells (Figure 1F; $n=4$). Immunoblots of KCNQ2 usually showed two bands, a sharp and faint 75 kDa band and a fuzzy 100 kDa band, which would correspond to unglycosylated and glycosylated KCNQ2 proteins respectively. The absence of biotinylation on a cytosolic marker protein, GFP, confirmed specificity of this surface labelling (Figure 1F, lower panel). Thus, the difference in current densities of these KCNQ2 mutants in CHO hm1 cells can be attributed to channel activity rather than the differences in the trafficking rates of the mutant channels. These results support the idea that the charge of S541 is key for channel activity.

PKC phosphorylation disrupts KCNQ2–calmodulin binding

Serine 541 is located in a distal segment of the two calmodulin-binding sites within cytoplasmic tail of the KCNQ2 subunit (Yus-Najera *et al*, 2002). Therefore, we reasoned that phosphorylation of this residue influences calmodulin binding. To test this hypothesis, we first performed immunoprecipitation of flag epitope-tagged wild-type or mutant KCNQ2 from cells cotransfected with V5 epitope-tagged calmodulin (Figure 2A) in a calcium-free condition. Immunoblot detection revealed that equivalent amounts of calmodulin coprecipitated with wild-type and KCNQ2 (S541A) proteins (Figure 2A, lanes 2 and 3). Conversely, a negligible amount of calmodulin was detected in KCNQ2

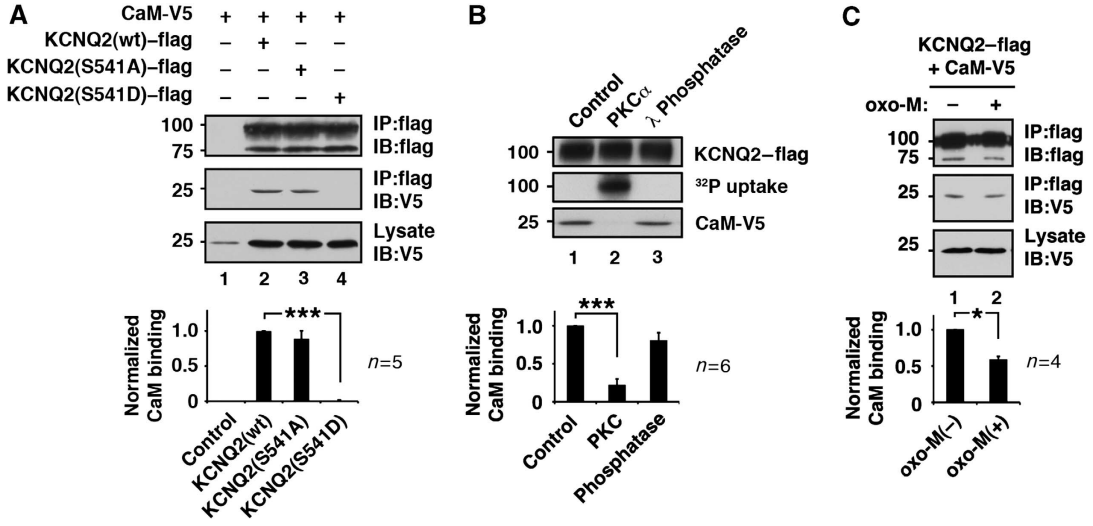

Figure 2 PKC phosphorylation interferes with KCNQ2–calmodulin interaction. (**A**) Calmodulin binding to KCNQ2 protein and its PKC site mutants. ***<0.001 by nonparametric ANOVA followed by Dunn's multiple comparisons test. (**B**) *In-vitro* phosphorylation of KCNQ2 protein by purified PKCα and its calmodulin binding capability. Phosphorylated KCNQ2 protein cannot bind calmodulin. Calmodulin binding of untreated control and dephosphorylated KCNQ2 are also shown. ***<0.001 by nonparametric ANOVA followed by Dunn's multiple comparisons test. (**C**) Oxo-M treatment reduced calmodulin binding to KCNQ2. *<0.05 by paired *t*-test. Error bars indicate s.e.m. Figure source data can be found with the Supplementary data.

(S541D) immune complexes (Figure 2A, lane 4; $n=5$). This suggests that phosphorylation of S541 may interfere with calmodulin binding. To test this directly, we performed an *in-vitro* phosphorylation using purified PKC and KCNQ2 prior to the calmodulin-binding assay (Figure 2B). KCNQ2–flag subunits were pulled down using anti-flag-conjugated beads and washed at high stringency. These KCNQ2-beads were then either left untreated, phosphorylated by purified PKC, or dephosphorylated by λ protein phosphatase. The incorporation of ^{32}P confirmed phosphorylation of the KCNQ2 protein (Figure 2B, middle blot, lane 2). The treated KCNQ2-beads were tested for calmodulin binding. CaM-V5 was used for this binding assay since it avoided detection of residual endogenous calmodulin that could remain during the KCNQ2 purification procedure. The PKC-phosphorylated KCNQ2 subunit bound a negligible amount of calmodulin (Figure 2B, lane 2; $n=6$) compared with untreated KCNQ2 controls (Figure 2B, lane 1; $n=6$). In contrast, calmodulin binding to the dephosphorylated KCNQ2 protein was robust and comparable to the untreated protein (Figure 2B, lane 3; $n=6$). Thus, PKC phosphorylation disrupts the KCNQ2–calmodulin interaction.

Next, we examined whether release of calmodulin from KCNQ2 subunits can be induced upon muscarinic receptor stimulation. CHO hm1 cells coexpressing KCNQ2–flag and CaM-V5 were treated with 3 μM oxo-M for 3 min. The KCNQ2 immune complexes were tested for calmodulin binding by immunoblot with V5 antibodies. As expected, oxo-M treatment decreased the coprecipitated calmodulin (Figure 2C; $n=4$).

To further examine whether muscarinic stimulation favours the dissociation of calmodulin from KCNQ channels in living cells, we performed intermolecular fluorescent resonance energy transfer (FRET) analyses (Figure 3). The FRET donor was monomeric cerulean, a brighter version of CFP (Shaner *et al*, 2005), tagged calmodulin (CaM–CFP). The FRET acceptor was monomeric citrine, a brighter version of YFP (Shaner *et al*, 2005), fused to KCNQ2 (KCNQ2–YFP). Fluorescent signals in the vicinity of the plasma membrane were detected by total internal reflection fluorescence (TIRF) microscopy (Steyer and Almers, 2001). These measurements revealed a higher FRET efficiency from the wild-type KCNQ2 (wt)–YFP and CaM–CFP pair over the control pair of KCNQ2 (wt)–YFP and CFP alone (Figure 3A and B; $n=96$ cells, $n=92$ cells, respectively). KCNQ2 (S541A) and CaM–CFP pair showed equivalent FRET signals to that of the wild-type pair (Figure 3A, middle; $104\pm8.2\%$ of wild-type, $n=101$). Importantly, a lower FRET efficiency was measured with the KCNQ2 (S541D)–YFP and CaM–CFP pair compared with wild-type KCNQ2–YFP (Figure 3A, right; $68.2\pm9.8\%$ of wild-type, $n=123$, $P<0.0001$). However, it is worthwhile to mention that the KCNQ2 (S541D) mutation weakened but did not completely eliminate the KCNQ2–calmodulin association since FRET efficiency with the CaM–CFP donor was elevated over that with the CFP donor alone (Figure 3A, right; $n=98$).

Application of the muscarinic agonist oxo-M also lowered the FRET efficiency for the KCNQ2–YFP + CaM–CFP pair (Figure 3B–F; $n=96$, $P<0.0001$). Since our coimmunoprecipitation experiments indicated that less KCNQ2 subunit bound CaM after oxo-M treatment (Figure 2C), we reasoned that the oxo-M responsive decrease in FRET signal was due to dissociation of CaM rather than change in dipole orientation. We next examined PKC involvement in calmodulin dissociation by suppressing PKC phosphorylation either by treating cells with BIS IV or by using KCNQ2 (S541A). Oxo-M induced FRET responses were suppressed to a similar degree in both KCNQ2 (S541A)–YFP + CaM–CFP (Figure 3F, green circles; $n=78$, $P<0.01$ at $t=2$ min) and BIS IV treated KCNQ2–YFP + CaM–YFP (Figure 3F, black circles; $n=121$, $P<0.01$ at $t=2$ min) compared with control responses (Figure 3F). These results imply that PKC phosphorylation of KCNQ2 induces dissociation of calmodulin in living cells.

Stable KCNQ2–calmodulin association is required for maintaining PIP2 affinity

Residues involved in PIP2 binding are scattered around the calmodulin-binding domains. One residue, histidine 328

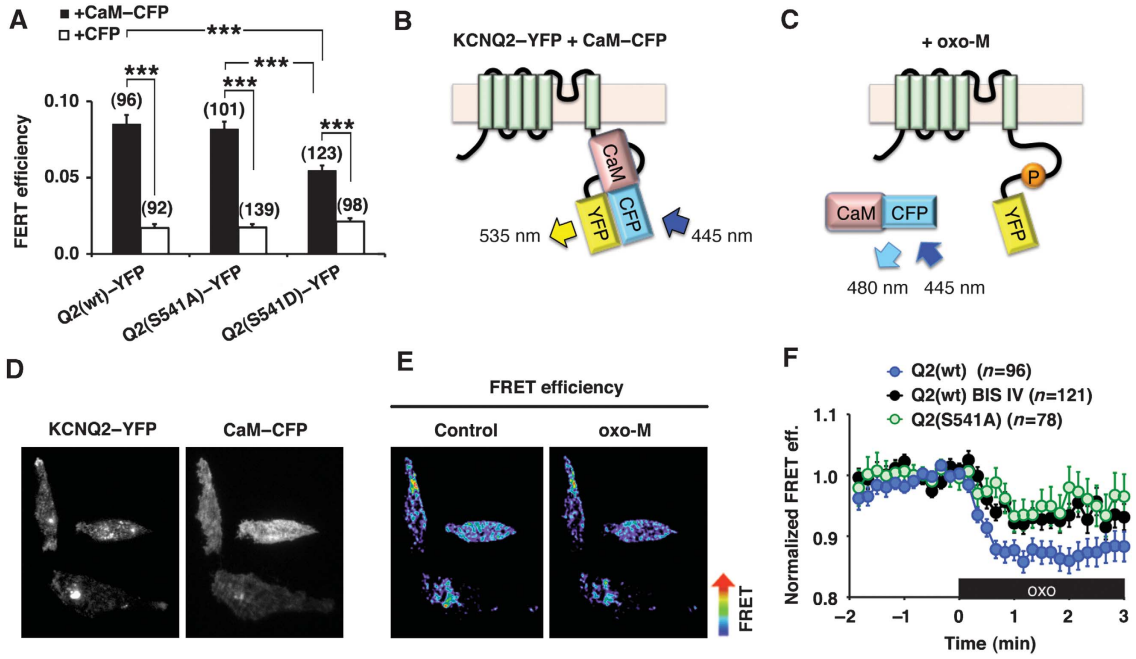

Figure 3 Muscarinic stimulation induces dissociation of calmodulin from the KCNQ2 channel complex in living cells. (**A**) Pooled FRET efficiencies. Increased FRET efficiencies were observed in the wild-type KCNQ2–YFP (Q2 (wt)–YFP) and calmodulin–CFP (CaM–CFP) pair over the control pair, KCNQ2–YFP and CFP alone. KCNQ2 (S541A)–YFP (Q2 (S541A)–YFP) and CaM–CFP pair showed equivalent FRET efficiency to the wild-type pair. KCNQ2 (S541D)–YFP (Q2 (S541D)–YFP) and CaM–CFP showed reduced FRET efficiency compared with that from the wild-type pair, but showed significant FRET efficiency over the CFP control. N indicates numbers of cells observed. *** <0.001 by nonparametric ANOVA followed by *t*-test. (**B**, **C**) Schematic representations of KCNQ2–YFP and calmodulin–CFP interaction in control (**B**) and oxo-M applied condition (**C**). (**D**) Fluorescent images from CHO hm1 cells coexpressing KCNQ2–YFP and CaM–CFP. (**E**) Pseudocolour images of the cells shown in (D) showing decrease in FRET efficiency after 3 μM oxo-M application. (**F**) Changes in FRET efficiencies of KCNQ2–YFP and CaM–CFP upon 3 μM oxo-M application. FRET efficiency of the wild-type KCNQ2–YFP + CaM–CFP (Q2 (wt), blue circles) was decreased upon stimulation with oxo-M. Pretreatment with BIS IV attenuated oxo-M responses (Q2 (wt) BIS IV, black circles). KCNQ2 (S541A) + CaM–CFP pair showed similar attenuated responses (Q2 (S541A), green circles). The black box indicates the presence of oxo-M. Error bars indicate s.e.m.

(Zhang *et al*, 2003), locates within the proximal segment of the calmodulin-binding site (residues 310–451 of the channel (Yus-Najera *et al*, 2002)). A cationic cluster domain, which is sandwiched between the two calmodulin-binding sites, provides an additional PIP2-binding domain (Hernandez *et al*, 2008). The location of these functional modules implies that calmodulin binding might affect PIP2–KCNQ2 interaction. To test this and in order to estimate the affinity of PIP2 for KCNQ2, we utilized neomycin, which is widely used to sequester PIP2 (Liscovitch *et al*, 1994; Haider *et al*, 2007; Suh and Hille, 2007). The inclusion of 300 μM neomycin in the patch pipette solution promoted a sustained decrease in the KCNQ2 current over a 10-min time course (Figure 4A and B; $n=10$). Neomycin-induced rundown of the KCNQ2 current was prevented by inclusion of the water-soluble PIP2 analogues, 500 μM diC4-PIP2 or 500 μM diC8-PIP2, in the pipette solution. (Figure 4B and D; $n=10$). Additional control experiments confirmed that extracellular application of 1 mM neomycin for 10 min had no effect on the KCNQ2 current (Figure 4C; $n=13$). This allowed us to conclude that neomycin sequesters PIP2 from the intracellular side of the plasma membrane. Furthermore, in some channels such as Kir2.1, the carbon chain of diC4-PIP2 is too short to maintain channel function (Rohacs *et al*, 1999). Our results suggest that KCNQ2 channel is less selective for acyl chain requirements (Figure 4D). This view is consistent with recent findings that KCNQ1 channel can be facilitated by diC4-PIP2 (Li *et al*, 2011) and that KCNQ2 channel activity is enhanced by a variety of negatively charged lipids (Telezhkin *et al*, 2012).

Next, we measured dose-responses for neomycin at 10 min time points after rupturing the membrane (Figure 4E). Wild-type and KCNQ2 (S541A) showed similar neomycin inhibition curves (see Supplementary Figure 1 for IC_{50} and Hill coefficients). In contrast, KCNQ2 (S541D) exhibited a higher sensitivity to neomycin, suggesting lower PIP2 affinity (Figure 4E, blue circles). To directly examine whether these channels have different PIP2 sensitivity, we included 500 μM diC8-PIP2 in the patch pipette solution and measured current augmentation 2 min after rupturing the plasma membrane (Figure 4F). Wild-type and KCNQ2 (S541A) did not show increase in current by diC8-PIP2, suggesting that endogenous PIP2 is at a saturating concentration. On the other hand, KCNQ2 (S541D) showed a 1.7 ± 0.4 fold increase ($n=17$, $P<0.01$ paired *t*-test). These results suggest that PKC phosphorylation of S541 can change not only calmodulin binding, but also the interaction with PIP2.

One remaining critical question is whether this change in PIP2 affinity is due to the reduced calmodulin binding or the conformational changes that are introduced into the cytoplasmic tail of the KCNQ2 subunit as a result of mutations at position S541. In order to resolve this important question, we analysed another calmodulin-deficient mutant, KCNQ2 (R353G), which has been identified in patients with benign familial neonatal convulsions (Etxeberria *et al*, 2008). As previously reported, KCNQ2 (R353G) exhibited a reduced

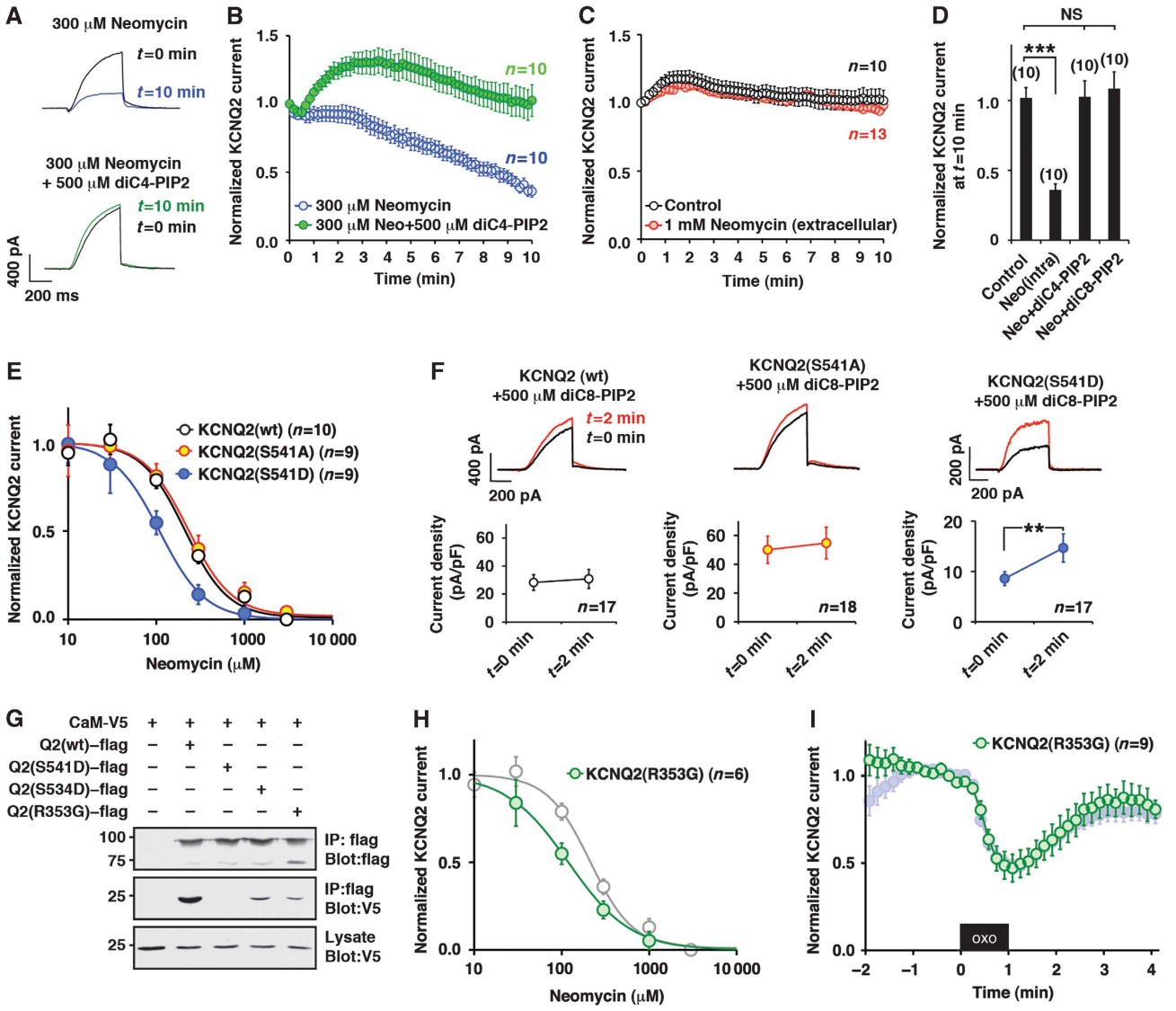

Figure 4 KCNQ2–calmodulin interaction determines PIP2 affinity of KCNQ2 channel. (**A**, **B**) Neomycin-induced rundown of KCNQ2 current and its prevention by diC4-PIP2. Current traces (**A**) and pooled data (**B**) show neomycin-induced rundown of KCNQ2 current (blue circles). This rundown was prevented by further addition of diC4-PIP2 in the patch pipette solution (green circles). KCNQ2 currents were normalized to KCNQ2 current at $t=0$. (**C**) Extracellular application of 1 mM neomycin (orange circles) did not affect KCNQ2 current compared with the control (open circles). (**D**) Histogram depicting KCNQ2 currents at $t=10$ min showing that both diC4-PIP2 and diC8-PIP2 are equally effective to restore KCNQ2 current rundown induced by neomycin. Values for control, intracellular neomycin and diC4-PIP2 are from (**B**, **C**). NS: not significant, *** <0.001 by nonparametric ANOVA followed by *t*-test. (**E**) Dose-response curves for neomycin measured at 10 min after rupturing the plasma membrane. Indicated concentration of neomycin was included in the patch pipette. Wild-type KCNQ2 (open circles, KCNQ2 (S541A) (yellow circles), and KCNQ2 (S541D) (blue circles) are shown. Solid lines show the best fits using one component Hill equation. See Supplementary Figure 1 for parameters. (**F**) Augmentation of KCNQ2 currents by diC8-PIP2 in the patch pipette solution. KCNQ2 (wt) and KCNQ2 (S541A) did not show apparent augmentations ($P>0.05$, paired *t*-test), while KCNQ2 (S541D) showed 1.7-fold increase (** <0.01, paired *t*-test), suggesting that endogenous PIP2 is not at saturating concentration for KCNQ2 (S541D). (**G**) Calmodulin binding of other KCNQ2 mutants including KCNQ2 (R353G) and KCNQ2 (S534D) compared with that of KCNQ2 (wt). (**H**) Dose response curve for neomycin of KCNQ2 (R353G) overlaid to that of KCNQ2 (wt) shown in (**E**) (grey circles). (**I**) KCNQ2 (R353G) (green circles) showed hyperreactivity to 0.1 μM oxo-M. Oxo-M response of KCNQ2 (S541D) shown in Figure 1D is also shown as a reference (shaded blue circles). Error bars indicate s.e.m.

current density compared with that of wild-type (15 ± 1.3 pA/pF, $n=57$) and reduced calmodulin binding compared with wild-type KCNQ2 channel (Figure 4G) (Etxeberria *et al*, 2008). Electrophysiological measurements using this mutant revealed an increased sensitivity towards neomycin, which was similar to that of KCNQ2 (S541D) (Figure 4H; Supplementary Figure 1; $n=6$). Interestingly, KCNQ2 (R353G) showed a hypersensitivity to oxo-M in a manner that was similar to the KCNQ2 (S541D) channel mutant (Figure 4I; $n=9$, $P<0.05$ compared with KCNQ2 (wt) shown in Figure 1D). These results show that distinct mechanism for disturbed calmodulin binding can result in similar PIP2 phenotype. One interpretation of these findings is that KCNQ2–calmodulin binding determines PIP2 affinity. However, these findings could be coincidence since observations were made with two mutants. To further minimize the risk of relating coincidental events, we analysed KCNQ2 (S534D), a secondary PKC phosphorylation site with a milder phenotype (Hoshi *et al*, 2003) (Figure 4G). Scattered plots from these mutants showed strong correlations among

KCNQ2–calmodulin binding, IC_{50} for neomycin and fold increase by diC8-PIP2 (Supplementary Figure 1). These results indicate that KCNQ2–calmodulin binding is closely related with PIP2 affinity.

PKC phosphorylation and muscarinic stimulation lower affinity towards PIP2

Since the KCNQ2 (S541D) phosphomimetic mutant enhances neomycin induced rundown of the current, we examined whether activation of cellular PKC can reduce the affinity of wild-type channel towards PIP2. KCNQ2-expressing cells were stimulated by phorbol-12,13-dibutyrate (PDBu) to activate PKC. To our surprise, 100 nM PDBu application alone had no effect on the KCNQ2 current in this condition (Figure 5A; $n=12$). Likewise, 100 μM neomycin alone had little effect on the KCNQ2 current (Figure 5B, open circles; $n=14$). When these two treatments were combined, however, application of PDBu could suppress KCNQ2 current (Figure 5B, black circles; $n=14$). This suggests that PKC-phosphorylated KCNQ2 channel becomes more sensitive to a reduction in the availability of PIP2 (Figure 5B and C). In contrast, KCNQ2 (S541A) channel did not show PDBu induced suppression even in the presence of neomycin, which suggests that PKC phosphorylation of S541 is key for this suppression (Figure 5C).

The next logical question was whether muscarinic stimulation decreases PIP2 affinity of the KCNQ2 channel. To test this hypothesis we used a metabolically stable PIP2 derivative, ms-PIP2, which is resistant to hydrolysis by PLC. We reasoned that if muscarinic suppression is exclusively mediated by PIP2 depletion, the stable ms-PIP2 derivative would sustain channel activity. Exchange of endogenous PIP2 for ms-PIP2 was favoured by maintaining a lower concentration of ATP (1 mM) in the patch pipette solution (Supplementary Figure 2). With 1 mM ATP in the pipette solution, KCNQ2 current showed significant rundown, which was prevented by higher ATP (4 mM) or further addition of 500 μM ms-PIP2 or 500 μM diC4-PIP2 in the pipette solution (Supplementary Figure 2). These results suggest that active KCNQ2 currents with 1 mM ATP in the pipette solution are maintained by exogenous PIP2. We examined muscarinic suppression of KCNQ2 currents in the presence of ms-PIP2 using 0.3 μM oxo-M. The wild-type KCNQ2 channel showed equivalent muscarinic suppression in both control (4 mM ATP) and ms-PIP2 supplemented condition (Figure 6A; $n=11$). The KCNQ2 (S541A) mutant, on the other hand, showed reduced muscarinic suppression compared with that of wild type (Figure 6B, open circle; $n=10$). Importantly, muscarinic suppression of KCNQ2 (S541A) was further attenuated in the presence of ms-PIP2 (Figure 6B and C; $n=9$). This implies that depletion of PIP2 serves as a dominant mechanism when the KCNQ2 subunit is not phosphorylated at Ser 541.

Finally, in order to examine this phenomenon under more physiological conditions, we evaluated whether ms-PIP2 can alter muscarinic suppression of the M-current in SCG neurons. The M-current is well known for its rundown during whole-cell patch clamp recordings, which we observed when we used a patch pipette solution with 1 mM ATP (Supplementary Figure 2). This rundown was partially prevented by raising the ATP concentration to 4 mM or by adding either 500 μM diC4-PIP2 or ms-PIP2 (Supplementary Figure 2).

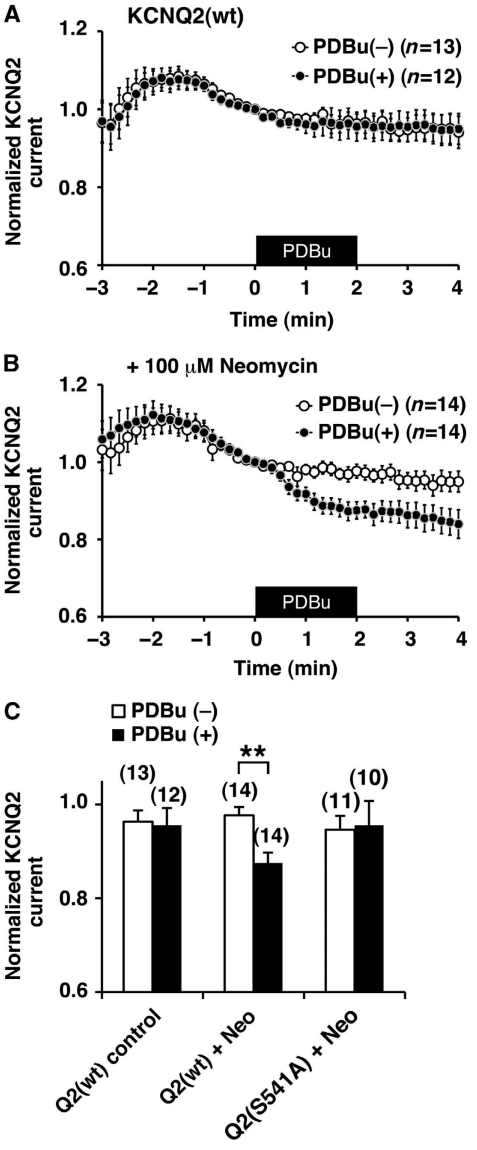

Figure 5 Activation of PKC sensitizes KCNQ2 current to sequestering of PIP2 by neomycin. (**A**) PDBu application onto wild-type KCNQ2 current had little effect. The black box indicates the presence of 100 nM PDBu. (**B**) PDBu application induced current suppression of wild-type KCNQ2 current when neomycin was included in the patch pipette solution. (**C**) Relative KCNQ2 current amplitudes at $t=2$ min from KCNQ2 (wt) without neomycin shown in (**A**) (left), in the presence of neomycin, Neo Q2 (wt), shown in (**B**) (middle), and KCNQ2 (S541A) in the presence of neomycin (right). $^{**}<0.01$ nonparametric ANOVA followed by *t*-test. Error bars indicate s.e.m.

When SCG neurons were stimulated by 0.1 μM oxo-M, the M-channel showed profound suppression in both the control (4 mM ATP), and ms-PIP2 supplied condition (1 mM ATP + ms PIP2) (Figure 6D; $n=17$). In contrast, when PKC was inhibited by BIS IV, ms-PIP2 could further attenuate the muscarinic suppression of the M-current (Figure 6E and F; $n=15$). These results indicate that PKC phosphorylation sensitizes the M-current for PIP2 reduction in SCG neurons.

Discussion

Understanding precisely how the M-current is modulated by neurotransmitters has been elusive since the initial identifica-

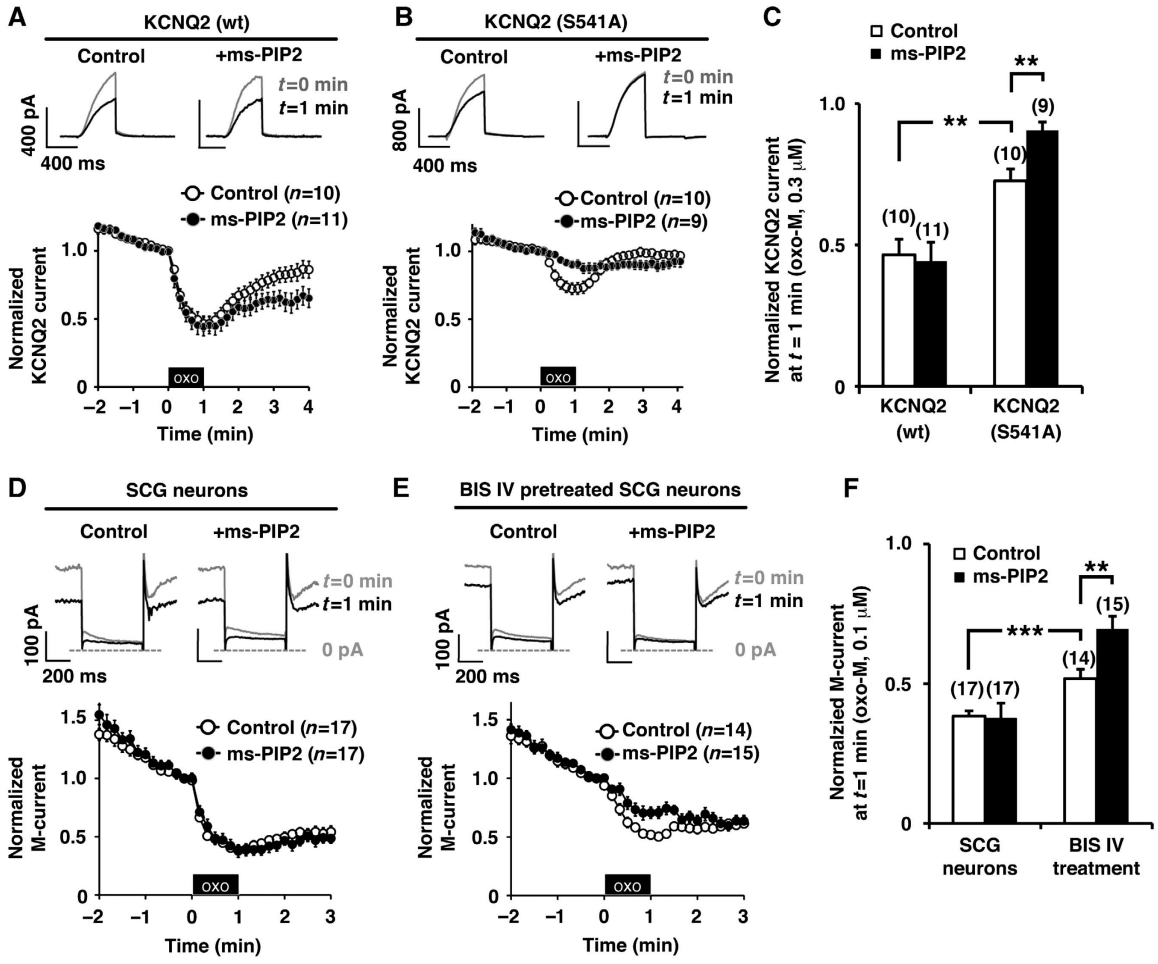

Figure 6 PKC phosphorylation sensitizes KCNQ2 channel and M-channel for reduction of PIP2 during muscarinic stimulation. (**A**) A PLC-resistant PIP2 analogue, ms-PIP2, did not disrupt oxo-M responses of wild-type KCNQ2 channel recorded by whole-cell patch clamp. The black box indicates the presence of 0.3 μM oxo-M. (**B**) Ms-PIP2 disrupted oxo-M responses of KCNQ2 (S541A) channel. (**C**) Pooled data of normalized KCNQ2 current at $t = 1$ min from (**A**, **B**) showing that exogenous ms-PIP2 had no effects on wild-type KCNQ2 channel in response to oxo-M. But for KCNQ2 (S541A) channel, ms-PIP2 attenuated the oxo-M response. $^{**}<0.01$ by nonparametric ANOVA followed by *t*-test. (**D**) Whole-cell patch-clamp recordings of the M-current from SCG neurons showing muscarinic suppression. Ms-PIP2 did not change the oxo-M response of the M-current. (**E**) Whole-cell patch-clamp recordings of the M-current from SCG neurons after pretreatment with 10 μM BIS IV. BIS IV treatment attenuated 0.1 μM oxo-M response, which was further suppressed by ms-PIP2. (**F**) Pooled data showing that exogenous ms-PIP2 attenuated oxo-M response when combined with BIS IV treatment. $^{**}<0.01$, $^{***}<0.001$ by nonparametric ANOVA followed by *t*-test. Error bars indicate s.e.m.

tion of this phenomenon by Brown and colleagues (Brown and Adams, 1980). The present study demonstrates how individual second messenger modulated signalling events are integrated during muscarinic suppression of the M-current. Our data suggest that modulation of this channel occurs in three steps as depicted in the model portrayed in Figure 7. First, PKC phosphorylation dissociates calmodulin from the KCNQ2 subunit; second, calmodulin-deficient KCNQ2 is less able to associate with PIP2; and third, the impaired ability to interact with PIP2 leads to a collapse of the channel pore (Hansen *et al*, 2011).

Pharmacological and electrophysiological analyses have been the primary approaches used to discern mechanisms of muscarinic suppression of the M-current. PKC activity was quickly identified as a candidate mediator of this important current modulation process (Higashida and Brown, 1986). However, this view was not widely accepted as some reports did not observe suppression of the M-current following activation of PKC with phorbol esters (Dutar and Nicoll, 1988; Marrion, 1997; Suh and Hille, 2006). Furthermore, treatment with staurosporine, a pharmacological inhibitor of PKC did not affect muscarinic suppression of these currents (Bosma and Hille, 1989; Shapiro *et al*, 2000). Some clarity is provided by evidence in Figures 1 and 2 showing that PKC phosphorylation of Ser541 on KCNQ2 suppresses the M-current. These findings tie in with previous reports that anchoring of PKC by AKAP79/150 modifies the susceptibility of this kinase to pharmacological agents including staurosporine (Hoshi *et al*, 2010; Smith and Hoshi, 2011). An important implication of the latter finding is that intracellular binding partners can change the pharmacological profile of certain protein kinases, which may explain why M-channels are insensitive to some PKC inhibitors. Although less well defined, a similar situation may apply to calmodulin binding. Several electrophysiological studies conclude that an increase in cytoplasmic calcium suppresses the M-current (Kirkwood and Lisman, 1992; Selyanko and Brown, 1996; Gamper and Shapiro, 2003). KCNQ2-bound calmodulin has been identified as a calcium sensor for the KCNQ2 subunit (Gamper and Shapiro, 2003). However, the molecular mechanism for calmodulin-dependent regulation remains controversial. One group argues that dissociation of

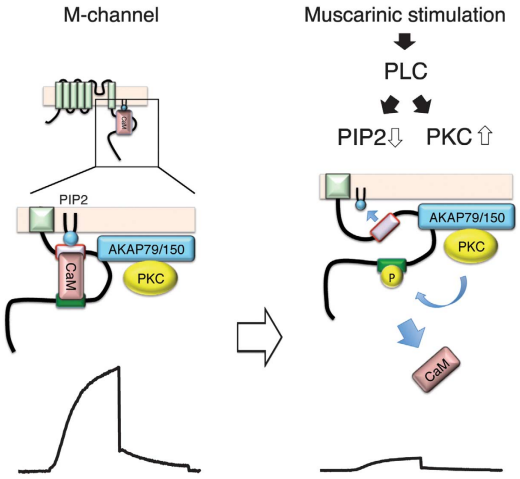

Figure 7 Schematic representation of KCNQ2 channel complex and a proposed channel complex rearrangement. KCNQ2 subunit of the M-channel tethers PIP2, CaM, AKAP79/150, and PKC. Activation of PLC by muscarinic stimulation depletes PIP2 and activates PKC, which phosphorylates KCNQ2 subunit. The phosphorylation of KCNQ2 at S541 located in the distal segment of the CaM-binding site induces dissociation of CaM from the KCNQ2 channel. Calmodulin-deficient KCNQ2 channel has lower affinity towards PIP2. Together with reduction of PIP2 induced by PLC activation, muscarinic stimulation generates profound suppression of the M-channel activity.

calmodulin from the KCNQ2 subunit corresponds to loss of channel function (Shahidullah *et al*, 2005), whereas others contend that conformational change of constitutively bound calmodulin regulates channel activity (Gamper and Shapiro, 2003; Bal *et al*, 2010). Although certain molecular details of this mechanism remain to be elucidated, our immunoprecipitation in Figure 2 and FRET-based analysis in Figure 3 show that calmodulin dissociation from the channel complex is related with suppression of the M-current.

Several studies concluded that PIP2 depletion is the key step for the muscarinic suppression of the M-current since rapid depletion and recovery of PIP2 correlate with M-current amplitude (Suh and Hille, 2002; Delmas and Brown, 2005; Winks *et al*, 2005; Suh *et al*, 2006). However, we would like to point out that DAG is rapidly produced by muscarinic stimulation since it is generated by equimolar conversion of PIP2 (Suh and Hille, 2006). In addition, we have previously demonstrated that AKAP79/150-dependent PKC phosphorylation follows almost identical time course with that of KCNQ2 current suppression upon muscarinic stimulation (Hoshi *et al*, 2010). Thus, despite a widely held view that depletion of PIP2 precedes other messengers, AKAP79-mediated PKC phosphorylation parallels the time course of KCNQ2 current modulation. In addition, PIP2 is recognized as an essential cofactor for a growing number of transporters and ion channels (Suh and Hille, 2008; Logothetis *et al*, 2010). A recent study shows that KCNQ2 is facilitated not only by PIP2, but also by a wide variety of negatively charged lipids (Telezhkin *et al*, 2012). Thus, the question arises as to how general depletion of PIP2 can form a selective pathway. An answer may lie in PKC phosphorylation of the M-channel, as our data in Figure 5 argue that the PKC-phosphorylated channel has reduced PIP2 affinity.

If PKC negatively regulates KCNQ2 current, why did PDBu application not suppress KCNQ2 current in some conditions? Our results indicate that whether PKC phosphorylation suppresses KCNQ2 currents depends on endogenous PIP2 levels. Interestingly, similar PIP2-dependent responses to PKC phosphorylation have been demonstrated for Kir3 channels (Keselman *et al*, 2007). In addition, PDBu is a mild agonist for cellular PKC activation. This phorbor ester induced ~50% of phosphorylation as compared with that induced by muscarinic stimulation (Smith and Hoshi, 2011). Furthermore, AKAP79/150 anchoring of PKC modifies the activation process (Faux and Scott, 1997). Since the KCNQ2 (S541D) phosphomimetic mutant showed reduced channel activity compared with that of wild-type, we believe that fully phosphorylated KCNQ2 should exhibit decreased channel activity over the physiological PIP2 concentration.

One critique to our model could be that we do not provide direct evidence that the loss of calmodulin induces reduction of PIP2 affinity. However, our mutant studies offer strong correlations between KCNQ2–calmodulin binding and PIP2 related events (Supplementary Figure 1), which suggests that these two events are closely related. In addition, our immunoprecipitation results suggest that PIP2 binding to KCNQ2 channel is not required for calmodulin binding since calmodulin binding is maintained after PIP2 is washed away during the procedure. Furthermore, Figure 2B showed that PKC phosphorylation leads to dissociation of calmodulin from KCNQ2. Based on these considerations, we think that calmodulin dissociation triggers reduction in PIP2 affinity. We propose that phosphorylation-induced rearrangement of the KCNQ channel complex may serve as a molecular framework for utilizing a common lipid molecule as a selective mediator. We would like to emphasize, though, that concomitant depletion of PIP2 upon muscarinic stimulation is critical for suppression of the M-current. We would like to propose that reduction of PIP2 affinity is equally important for the process.

The KCNQ2 gene was first discovered as an epilepsy gene (Jentsch, 2000). Interestingly, one mutant linked to familial epilepsy used in this study showed a low affinity to PIP2 as well as hyperreactivity to muscarinic stimulation. To date, the pathogenesis of epilepsy by these mutations has been attributed to poor membrane trafficking (Jentsch, 2000; Etxeberria *et al*, 2008). However, on the basis of our findings in Figure 4 we can speculate that low channel activity due to low PIP2 affinity as well as hyperreactivity to muscarinic stimulation would also contribute to pathogenesis of these calmodulin-deficient KCNQ2 mutations.

Finally, the conclusions of this work emphasize the significance of signalling complexes as a point of convergence and integration of these overlapping modulatory signals. In a broader context, our data predict that the seemingly redundant actions of PKC, calmodulin, and PIP2 act synergistically to create a fail-safe mechanism for M-current suppression that caused the enigma in the field. These elaborate layers of M-current regulation are mandated by the need to tightly regulate neuronal excitability.

Materials and methods

Materials and reagents

Anti-V5 epitope monoclonal antibody, mammalian expression vectors (pZeoSV, pcDNA3.1/V5 directional topo expression kit) were purchased from Life Technologies (Carlsbad, CA, USA). Anti-flag-conjugated resin, horse radish peroxidase conjugated anti-flag antibody, amphotericin B, phorbol-12,13-dibutyrate (PDBu) and

2,3-bis (1H-Indol-3-yl)maleimide (bisindolylmaleimide IV, BIS IV) were purchased from Sigma-Aldrich (St Louis, MO, USA). Phosphatidylinositol 4,5-bisphosphate diC4 (diC4-PIP2), phosphatidylinositol 4,5-bisphosphate diC8 (diC8-PIP2) and PtdIns (4,5)P2 α-fluorophosphonate diC8 (ms-PIP2) were purchased from Echelon biosciences (Salt Lake City, UT, USA). Sulfo-NHS-LC-biotin and neutravidin resin were purchased from Thermo scientific (Rockford, IL, USA). Purified PKCα was purchased from EMD biosciences (Rockland, MA, USA). Lambda protein phosphatase was purchased from New England Biolab (Ipswich, MA, USA). Trans-IT1 reagent was purchased from Mirus Bio (Madison, WI, USA).

Expression constructs

The wild-type flag-tagged rat KCNQ2 construct in pZeoSV has been described (Hoshi *et al*, 2003, 2005). KCNQ2 mutations (S541A, S541D and R353G) were generated by QuickChange II XL site-directed mutagenesis (Agilent Technologies, San Diego, CA, USA). The V5 epitope-tagged calmodulin construct was obtained by RT–PCR from rat brain cDNA and subcloning into pcDNA/V5 vector. All PCR derived constructs were verified by sequencing.

Cell culture and transfection

HEK293 cells were grown in Dulbecco's modified Eagle medium with 10% fetal bovine serum. CHO hm1 cells were grown in alpha modified Eagle medium with 5% fetal bovine serum and 500 μg/ml G418 sulphate. SCG neurons were isolated from 14- to 19-day-old rats and cultured as described previously (Hoshi *et al*, 2003). Acquisition of primary cultures was under the regulation of the Institutional Animal Care and Use Committee at University of California, Irvine.

Immunoprecipitation

Flag-tagged KCNQ2 channel complexes were immunoprecipitated from one 10 cm dish of HEK293 cells that had been transfected with 1 μg pZeoSV/KCNQ2–flag and 1 μg pcDNA3/CaM-V5 using Trans-IT1 reagent. Cells were harvested 48 hr after transfection and lysed in 500 μl HSE buffer (150 mM NaCl, 5 mM EDTA, 5 mM EGTA, 20 mM HEPES (pH 7.4), 1% Triton X-100 and complete protease inhibitor cocktail (Roche)). Supernatants were incubated with anti-flag antibody-conjugated resin. Following overnight incubation at 4°C, immunoprecipitates were washed in HSE buffer. Bound proteins were analysed by SDS–PAGE and immunoblotted with HRP-conjugated anti-flag antibody and anti-V5 antibody.

Surface labelling

Flag-tagged KCNQ2 channels were transiently expressed in CHO hm1 cells. Cells were washed twice with ice-cold phosphate-buffered saline solution (PBS) followed by incubation with sulfo-NHS-LC-biotin for 30 min at 4°C. The treated cells were further washed twice with PBS containing 100 mM glycine. Cells were then lysed in HSE buffer with complete protease inhibitor. Biotinylated proteins were purified by neutravidin resin and detected by immunoblots using anti-flag antibody.

In-vitro phosphorylation and binding assay

Flag-tagged KCNQ2 channels were purified from transiently transfected HEK293 cells by immunoprecipitation combined with high salt/calcium wash. Cells were in a lysis buffer (150 mM NaCl, 5 mM EDTA, 5 mM EGTA, 10 mM HEPES (pH 7.4), 1% CHAPS and complete protease inhibitor cocktail) and incubated with anti-flag-conjugated resin. KCNQ2-bound resin was washed twice with lysis buffer, twice with 650 mM NaCl, 500 μM $CaCl_2$, 1% CHAPS, 10 mM HEPES (pH 7.4), and twice with 150 mM NaCl, 500 μM $CaCl_2$, 1% CHAPS, 10 mM HEPES (pH 7.4). Calcium washes reduced KCNQ2-bound calmodulin to an undetectable level. KCNQ2-resin was then phosphorylated with PKCα in a phosphorylation buffer (150 mM NaCl, 500 μM $CaCl_2$, 100 nM PDBu, 200 μM ATP (7.4 MBq [γ^{32}P]-ATP), 10 mM HEPES (pH 7.4)). After washes with the phosphorylation buffer, purified CaM-V5 was added. CaM-V5 was purified from transiently transfected HEK293 cells using Ni-NTA resin. CaM-resin was washed with lysis buffer without EDTA and EGTA, and eluted by lysis buffer with 50 mM NaF, 1 mM $NaVO_4$, and 100 nM microcystin.

Electrophysiological measurements

Patch-clamp recordings were performed at room temperature on isolated cells using an Axopatch 200B patch-clamp amplifier (Molecular Devices, Sunnyvale, CA, USA). Signals were sampled at 2 kHz, filtered at 1 kHz, and acquired using pClamp software (version 7, Molecular Devices). Perforated patch clamp used in Figure 1A and B has been described (Hoshi *et al*, 2003, 2005). For whole-cell clamp recordings, cells were perfused with a solution containing 144 mM NaCl, 5 mM KCl, 2 mM $CaCl_2$, 0.5 mM $MgCl_2$, 10 mM glucose, 10 mM HEPES (pH 7.4). Patch pipettes (2–4 MΩ) were filled with intracellular solution containing 135 mM potassium aspartate, 2 mM $MgCl_2$, 3 mM EGTA, 1 mM $CaCl_2$ (free calcium 90 nM), 4 mM ATP, 0.1 mM GTP 10 mM, HEPES (pH 7.2) unless indicated otherwise. KCNQ2 channels were activated from a holding potential of −80 mV by two-step test pulses to −10 mV followed by −70 mV with 500 ms duration for each step. KCNQ2 currents were measured at the end of the −10 mV step. Amplitudes of the M-currents were measured as deactivating currents during 500-ms test pulses to −60 mV from a holding potential of −30 mV. For pretreatment with 10 μM BIS IV, cells were incubated >5 min and BIS IV was present throughout the corresponding experiments. *P*-values for statistics were calculated using InStat software (Graphpad, San Diego, CA, USA) and Excel (Microsoft, Redmond, WA, USA).

Live cell imaging

Live cell imaging and FRET imaging were performed essentially as described previously (Smith and Hoshi, 2011). Briefly, fluorescence emission was acquired using an inverted microscope IX-81 (Olympus Tokyo, Japan) and ImageEM CCD camera (Hamamatsu photonics, Shizuoka, Japan) controlled by MetaMorph 7.6.3 (Molecular Devices, Sunnyvale, CA, USA). The excitation light for TIRF experiments, a 445-nm diode laser (Coherent, Santa Clara, CA, USA) and 515 nm diode-pumped solid-state laser (Cobolt, Stockholm, Sweden) with an acousto-optic tunable filter were used with a TIRF module (Olympus, Tokyo, Japan). Dual-emission images were obtained simultaneously through a dual-view module (Photometrics, Tuscon, AZ, USA) with ET535/30m, ET480/40m emission filters and a T505lpxr dichroic mirror (Chroma Technology, Bellows Falls, VT, USA). Exposure time was 100 ms; images were taken every 10 s. Apparent FRET efficiency was calculated from the three fluorescent channels as described (van Rheenen *et al*, 2004; Saneyoshi *et al*, 2008). Parameters for calculating sensitized FRET were updated every 3 h using CHO cells expressing either mCitrine or mCerulean alone.

Supplementary data

Supplementary data are available at *The EMBO Journal* Online (http://www.embojournal.org).

Acknowledgements

We thank Dr Hee Jung Chung (University of Illinois) for human KCNQ2 (A343D) and KCNQ2 (R353G) constructs. This work was supported by NIH Grants NS067288 to NH and GM48231 to JDS.

Author contributions: AK, SK, IMS, DG and NH designed and performed the experiments. NH, AK, IMS, LKL and JDS analysed the data and wrote the manuscript.

Conflict of interest

The authors declare that they have no conflict of interest.

References

Bal M, Zhang J, Hernandez CC, Zaika O, Shapiro MS (2010) Ca2+/calmodulin disrupts AKAP79/150 interactions with KCNQ (M-Type) K+ channels. *J Neurosci* **30:** 2311–2323

Bosma MM, Hille B (1989) Protein kinase C is not necessary for peptide-induced suppression of M current or for desensitization of the peptide receptors. *Proc Natl Acad Sci USA* **86:** 2943–2947

Brown DA, Adams PR (1980) Muscarinic suppression of a novel voltage-sensitive K+ current in a vertebrate neurone. *Nature* **283:** 673–676

Buzsaki G (2002) Theta oscillations in the hippocampus. *Neuron* **33:** 325–340

Cooper EC, Jan LY (1999) Ion channel genes and human neurological disease: recent progress, prospects, and challenges. *Proc Natl Acad Sci USA* **96:** 4759–4766

Delmas P, Brown DA (2005) Pathways modulating neural KCNQ/M (Kv7) potassium channels. *Nat Rev Neurosci* **6:** 850–862

Dutar P, Nicoll RA (1988) Classification of muscarinic responses in hippocampus in terms of receptor subtypes and second-messenger systems: electrophysiological studies in vitro. *J Neurosci* **8:** 4214–4224

Etxeberria A, Aivar P, Rodriguez-Alfaro JA, Alaimo A, Villace P, Gomez-Posada JC, Areso P, Villarroel A (2008) Calmodulin regulates the trafficking of KCNQ2 potassium channels. *FASEB J* **22:** 1135–1143

Faux MC, Scott JD (1997) Regulation of the AKAP79-protein kinase C interaction by Ca2+/Calmodulin. *J Biol Chem* **272:** 17038–17044

Gamper N, Shapiro MS (2003) Calmodulin mediates Ca2+-dependent modulation of M-type K+ channels. *J Gen Physiol* **122:** 17–31

George MS, Abbott LF, Siegelbaum SA (2009) HCN hyperpolarization-activated cation channels inhibit EPSPs by interactions with M-type K (+) channels. *Nat Neurosci* **12:** 577–584

Haider S, Tarasov AI, Craig TJ, Sansom MS, Ashcroft FM (2007) Identification of the PIP2-binding site on Kir6.2 by molecular modelling and functional analysis. *EMBO J* **26:** 3749–3759

Hansen SB, Tao X, MacKinnon R (2011) Structural basis of PIP2 activation of the classical inward rectifier K+ channel Kir2.2. *Nature* **477:** 495–498

Hernandez CC, Zaika O, Shapiro MS (2008) A carboxy-terminal inter-helix linker as the site of phosphatidylinositol 4,5-bisphosphate action on Kv7 (M-type) K+ channels. *J Gen Physiol* **132:** 361–381

Higashida H, Brown DA (1986) Two polyphosphatidylinositide metabolites control two K+ currents in a neuronal cell. *Nature* **323:** 333–335

Hoshi N, Langeberg LK, Gould CM, Newton AC, Scott JD (2010) Interaction with AKAP79 modifies the cellular pharmacology of PKC. *Mol Cell* **37:** 541–550

Hoshi N, Langeberg LK, Scott JD (2005) Distinct enzyme combinations in AKAP signalling complexes permit functional diversity. *Nat Cell Biol* **7:** 1066–1073

Hoshi N, Zhang JS, Omaki M, Takeuchi T, Yokoyama S, Wanaverbecq N, Langeberg LK, Yoneda Y, Scott JD, Brown DA, Higashida H (2003) AKAP150 signaling complex promotes suppression of the M-current by muscarinic agonists. *Nat Neurosci* **6:** 564–571

Hu H, Vervaeke K, Graham LJ, Storm JF (2009) Complementary theta resonance filtering by two spatially segregated mechanisms in CA1 hippocampal pyramidal neurons. *J Neurosci* **29:** 14472–14483

Jentsch TJ (2000) Neuronal KCNQ potassium channels: physiology and role in disease. *Nat Rev Neurosci* **1:** 21–30

Keselman I, Fribourg M, Felsenfeld DP, Logothetis DE (2007) Mechanism of PLC-mediated Kir3 current inhibition. *Channels (Austin)* **1:** 113–123

Kirkwood A, Lisman JE (1992) Action potentials produce a long-term enhancement of M-current in frog sympathetic ganglion. *Brain Res* **580:** 281–287

Li Y, Zaydman MA, Wu D, Shi J, Guan M, Virgin-Downey B, Cui J (2011) KCNE1 enhances phosphatidylinositol 4,5-bisphosphate (PIP2) sensitivity of IKs to modulate channel activity. *Proc Natl Acad Sci USA* **108:** 9095–9100

Liscovitch M, Chalifa V, Pertile P, Chen CS, Cantley LC (1994) Novel function of phosphatidylinositol 4,5-bisphosphate as a cofactor for brain membrane phospholipase D. *J Biol Chem* **269:** 21403–21406

Logothetis DE, Petrou VI, Adney SK, Mahajan R (2010) Channelopathies linked to plasma membrane phosphoinositides. *Pflugers Arch* **460:** 321–341

Marrion NV (1997) Control of M-current. *Annu Rev Physiol* **59:** 483–504

Pan Z, Kao T, Horvath Z, Lemos J, Sul JY, Cranstoun SD, Bennett V, Scherer SS, Cooper EC (2006) A common ankyrin-G-based mechanism retains KCNQ and NaV channels at electrically active domains of the axon. *J Neurosci* **26:** 2599–2613

Peters HC, Hu H, Pongs O, Storm JF, Isbrandt D (2005) Conditional transgenic suppression of M channels in mouse brain reveals functions in neuronal excitability, resonance and behavior. *Nat Neurosci* **8:** 51–60

Rohacs T, Chen J, Prestwich GD, Logothetis DE (1999) Distinct specificities of inwardly rectifying K (+) channels for phosphoinositides. *J Biol Chem* **274:** 36065–36072

Saneyoshi T, Wayman G, Fortin D, Davare M, Hoshi N, Nozaki N, Natsume T, Soderling TR (2008) Activity-dependent synaptogenesis: regulation by a CaM-kinase kinase/CaM-kinase I/betaPIX signaling complex. *Neuron* **57:** 94–107

Selyanko AA, Brown DA (1996) Intracellular calcium directly inhibits potassium M channels in excised membrane patches from rat sympathetic neurons. *Neuron* **16:** 151–162

Shah MM, Migliore M, Brown DA (2011) Differential effects of Kv7 (M-) channels on synaptic integration in distinct subcellular compartments of rat hippocampal pyramidal neurons. *J Physiol* **589**(Pt 24): 6029–6038

Shah MM, Migliore M, Valencia I, Cooper EC, Brown DA (2008) Functional significance of axonal Kv7 channels in hippocampal pyramidal neurons. *Proc Natl Acad Sci USA* **105:** 7869–7874

Shahidullah M, Santarelli LC, Wen H, Levitan IB (2005) Expression of a calmodulin-binding KCNQ2 potassium channel fragment modulates neuronal M-current and membrane excitability. *Proc Natl Acad Sci USA* **102:** 16454–16459

Shaner NC, Steinbach PA, Tsien RY (2005) A guide to choosing fluorescent proteins. *Nat Methods* **2:** 905–909

Shapiro MS, Roche JP, Kaftan EJ, Cruzblanca H, Mackie K, Hille B (2000) Reconstitution of muscarinic modulation of the KCNQ2/KCNQ3 K (+) channels that underlie the neuronal M current. *J Neurosci* **20:** 1710–1721

Smith IM, Hoshi N (2011) ATP competitive protein kinase C inhibitors demonstrate distinct state-dependent inhibition. *PLoS One* **6:** e26338

Steyer JA, Almers W (2001) A real-time view of life within 100 nm of the plasma membrane. *Nat Rev Mol Cell Biol* **2:** 268–275

Suh BC, Hille B (2002) Recovery from muscarinic modulation of M current channels requires phosphatidylinositol 4,5-bisphosphate synthesis. *Neuron* **35:** 507–520

Suh BC, Hille B (2006) Does diacylglycerol regulate KCNQ channels? *Pflugers Arch* **453:** 293–301

Suh BC, Hille B (2007) Electrostatic interaction of internal Mg2+ with membrane PIP2 Seen with KCNQ K+ channels. *J Gen Physiol* **130:** 241–256

Suh BC, Hille B (2008) PIP2 is a necessary cofactor for ion channel function: how and why? *Annu Rev Biophys* **37:** 175–195

Suh BC, Inoue T, Meyer T, Hille B (2006) Rapid chemically induced changes of PtdIns (4,5)P2 gate KCNQ ion channels. *Science* **314:** 1454–1457

Telezhkin V, Reilly JM, Thomas AM, Tinker A, Brown DA (2012) Structural requirements of membrane phospholipids for M-type potassium channel activation and binding. *J Biol Chem* **287:** 10001–10012

van Rheenen J, Langeslag M, Jalink K (2004) Correcting confocal acquisition to optimize imaging of fluorescence resonance energy transfer by sensitized emission. *Biophys J* **86:** 2517–2529

Winks JS, Hughes S, Filippov AK, Tatulian L, Abogadie FC, Brown DA, Marsh SJ (2005) Relationship between membrane phosphatidylinositol-4,5-bisphosphate and receptor-mediated inhibition of native neuronal M channels. *J Neurosci* **25:** 3400–3413

Yus-Najera E, Santana-Castro I, Villarroel A (2002) The identification and characterization of a noncontinuous calmodulin-binding site in noninactivating voltage-dependent KCNQ potassium channels. *J Biol Chem* **277:** 28545–28553

Zhang H, Craciun LC, Mirshahi T, Rohacs T, Lopes CM, Jin T, Logothetis DE (2003) PIP (2) activates KCNQ channels, and its hydrolysis underlies receptor-mediated inhibition of M currents. *Neuron* **37:** 963–975

